




UV-assisted mechanoluminescence properties of SrAl₂O₄:(Eu,Dy) for impact sensing

Qinan Mao^{1,*} , Zhian Chen¹, Zhenguo Ji^{1,*}, and Junhua Xi¹

¹ College of Materials and Environmental Engineering, Hangzhou Dianzi University, Hangzhou 310018, People's Republic of China

Received: 4 January 2017

Accepted: 25 March 2017

Published online:
17 April 2017

© Springer Science+Business
Media New York 2017

ABSTRACT

SrAl₂O₄:(Eu,Dy) is one of the most promising mechanoluminescence materials that have potential applications in stress sensing, lighting, imaging and energy conversion. However, the ML intensity decays with the afterglow time of SrAl₂O₄:(Eu,Dy), which hampers its application in the real world. Here, the mechanoluminescence property of SrAl₂O₄:(Eu,Dy) was investigated by impact of a load. A method was proposed to overcome the drawback of the mechanoluminescence decay behavior associated with the afterglow time. During the measurement of mechanoluminescence, continuous UV irradiation on SrAl₂O₄:(Eu,Dy) can effectively realize steady-state mechanoluminescence that is independent of the afterglow time. The underlying mechanism is discussed in this paper.

Introduction

Mechanoluminescence (ML) is a phenomenon of light emission resulting from mechanical action on a solid. Depending on the nature of the mechanical stimulus, ML can be divided into three categories: elasto-ML, plasto-ML and fracto-ML [1]. Elasto-ML is light emission induced by elastic deformation. So, the process is non-destructive and reproducible. With those advantages, elasto-ML has shown potential applications for stress sensing, lighting, imaging and energy conversion [2–8].

In recent years, much effort has been expended on elasto-ML. However, only a few materials are found to exhibit intensive elasto-ML, which are suitable for the potential applications [9, 10]. Among them, SrAl₂O₄:(Eu,Dy) is one of the most promising

elasto-ML materials and has been extensively studied since the first report on the elasto-ML property of SrAl₂O₄:Eu in 1999 [11]. The ML of SrAl₂O₄:(Eu,Dy) phosphor can be observed in day light with naked eyes and is relatively easier to be detected by characterization apparatus. In the elastic deformation region, the ML intensity of SrAl₂O₄:(Eu,Dy) shows a good linear relationship with the deformation rate, impact energy and torsion [12–15]. Based on that, the phosphor has been successfully used to measure the stress and visualize the stress distribution in solids [16–20].

Even so, the practical application of SrAl₂O₄:(Eu,Dy) as stress-sensing devices still remains challenges. SrAl₂O₄:(Eu,Dy) phosphor is widely known as a persistent luminescence material that can emit light for several tens of hours after the end of excitation.

Address correspondence to E-mail: maoqinan@hdu.edu.cn; jizg@hdu.edu.cn

Generally, the persistent luminescence of $\text{SrAl}_2\text{O}_4:(\text{Eu},\text{Dy})$ (Eu,Dy) is related to the charge carriers caught by the so-called traps located during excitation. After the excitation ceases, the trapped charge carriers are gradually released from the traps, return to the activators and finally produce luminescence [21]. Similarly, the ML of $\text{SrAl}_2\text{O}_4:(\text{Eu},\text{Dy})$ is also believed to attribute to the trapped charge carriers which can be released by mechanical stimulus and then recombine with the luminescence center, resulting in photoemission [16]. Therefore, it is easy to deduce that the concentration of the trapped charge carriers is one of the factors affecting the intensity of elasto-ML of $\text{SrAl}_2\text{O}_4:(\text{Eu},\text{Dy})$ [16]. However, the concentration of the trapped charge carriers decreases as the time elapses after the excitation, due to the thermal release of the trapped charge carriers. Accordingly, the intensity of ML is also related to the afterglow decay time elapsed until the onset of mechanical stimulus [22, 23]. This fact makes difficulty in qualitative stress measurement and hampers the application of $\text{SrAl}_2\text{O}_4:(\text{Eu},\text{Dy})$ as a stress-sensing material in the real world.

In this paper, we found an effective way to solve the problem that the ML of $\text{SrAl}_2\text{O}_4:(\text{Eu},\text{Dy})$ was affected by the afterglow decay time. Steady-state and enhanced ML of $\text{SrAl}_2\text{O}_4:(\text{Eu},\text{Dy})$ was achieved by the assistance of continuous UV irradiation.

Experimental

In this study, a commercial $\text{SrAl}_2\text{O}_4:(\text{Eu},\text{Dy})$ phosphor (Shenzhen Yaodexing Technology Ltd., KYD-7) was used as the elasto-ML material. The $\text{SrAl}_2\text{O}_4:(\text{Eu},\text{Dy})$ powder mixed thoroughly with an optical epoxy resin (Truer MC003) in a weight ratio of 1:1. The composite was coated onto polycarbonate substrates by the doctor blade method [24] and then cured in the oven at 65 °C for 2 h to obtain the ML-sensing film with a thickness of 350 μm .

The photoluminescence of the ML-sensing film was characterized by a Shimadzu RF-5301PC fluorescence spectrometer. The ML of $\text{SrAl}_2\text{O}_4:(\text{Eu},\text{Dy})$ was measured by a homemade setup as shown in Fig. 1. The measurement of ML was carried out in an optical enclosure to shield against ambient light. The ML film sample was placed on a plate that inclined 45° to the horizontal line. The impact force applied on the sample was realized by dropping a stainless steel ball

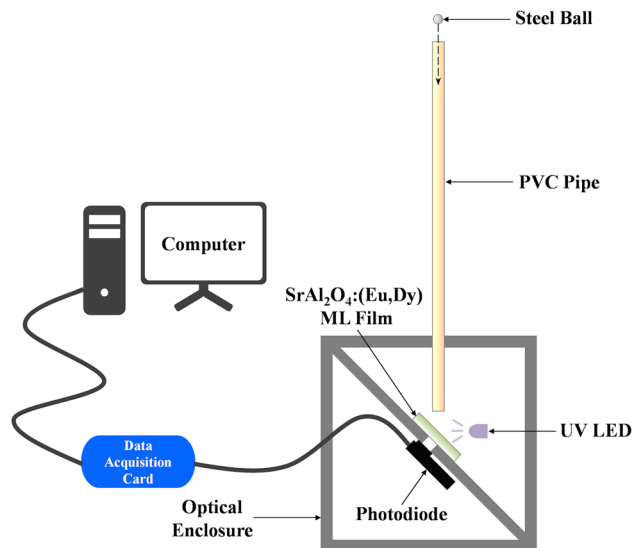


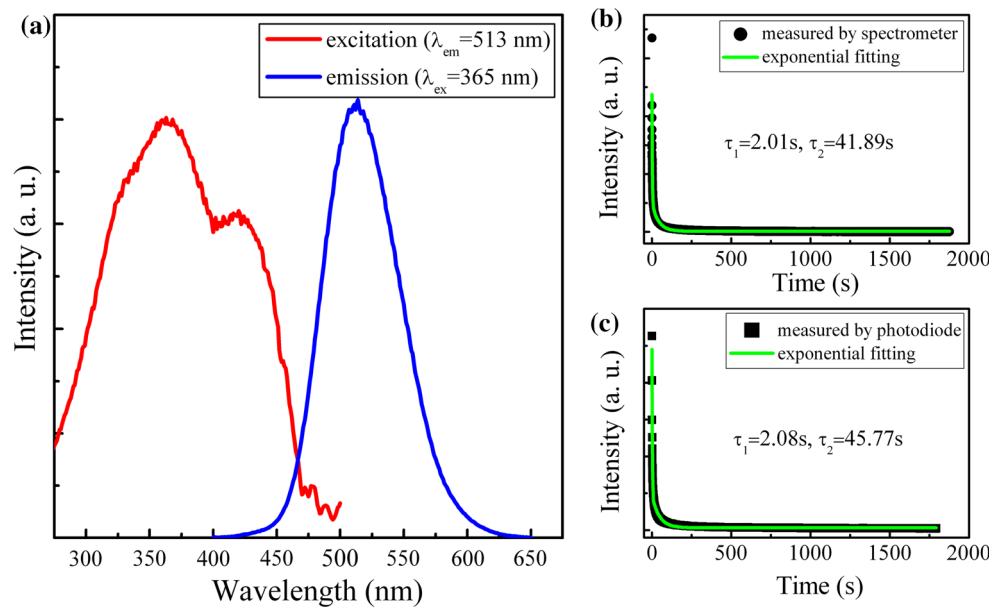
Figure 1 Schematic diagram of the homemade setup for measurement of impact-induced ML.

(mass, 13.6 g; diameter, 15 mm) from a fixed height through a PVC pipe onto the ML film. The ML intensity of the film was measured using an amplified Si photodiode detector (Thorlabs PDA100A). The output voltage of the Si photodiode detector was collected via a PC-based data acquisition card (Art Technology USB 2813).

Results and discussion

Figure 2a shows the excitation and emission spectra of $\text{SrAl}_2\text{O}_4:(\text{Eu},\text{Dy})$ ML film. The excitation spectrum contains a broad band with peaks at about 365 nm and 420 nm. Under 365 nm excitation, a broad emission centered at 513 nm was observed. The emission band can be ascribed to $4f^65d \rightarrow 4f^7$ electronic transition of Eu^{2+} ions in $\text{SrAl}_2\text{O}_4:(\text{Eu},\text{Dy})$ phosphor. Besides, the photoluminescent property of the epoxy resin film without $\text{SrAl}_2\text{O}_4:(\text{Eu},\text{Dy})$ powder was also investigated. No emission was detected by the fluorescence spectrometer. Figure 2b, c shows the afterglow decay curves of $\text{SrAl}_2\text{O}_4:(\text{Eu},\text{Dy})$ ML film measured by the fluorescence spectrometer and the amplified photodiode, respectively. The persistent luminescence process usually contains a rapid decay process and a slow decay process, which can be described by a double exponential equation. The equation is shown as follows [25]

Figure 2 **a** Excitation and emission spectra of the $\text{SrAl}_2\text{O}_4:(\text{Eu},\text{Dy})$ film. Afterglow decay curves of the $\text{SrAl}_2\text{O}_4:(\text{Eu},\text{Dy})$ film measured by **b** the fluorescence spectrometer and **c** the amplified photodiode.



$$I = I_0 + I_1 \exp\left(-\frac{t}{\tau_1}\right) + I_2 \exp\left(-\frac{t}{\tau_2}\right) \quad (1)$$

where I represents the phosphorescent intensity; I_0 , I_1 and I_2 are three constants; t represents the time; τ_1 and τ_2 are decay constants which decide the decay rate for the rapid and the slow exponential decay components, respectively. By fitting the decay curves using Eq. (1), the values of the decay constants τ_1 and τ_2 are 2.01 and 41.89 s for the ML film measured by the fluorescence spectrometer, and 2.08 and 45.77 s for the ML film measured by the amplified photodiode. The result obtained by the amplified photodiode is in good agreement with that obtained by the fluorescence spectrometer, which means that the detector can well reflect the actual persistent luminescence process.

Figure 3 presents the impact-induced ML intensity of $\text{SrAl}_2\text{O}_4:(\text{Eu},\text{Dy})$ film after different afterglow decay time. In this experiment, the ML films were pre-irradiated by 365 nm UV LED (voltage = 3.2 V; current = 0.10 A) for 5 min before the ML measurement. The impacts were applied on the ML films after various decay times (30, 60, 90, 120, 150 s). The typical ML curves are shown in the inset of Fig. 3. The baselines of the curves result from the persistent luminescence decay of the $\text{SrAl}_2\text{O}_4:(\text{Eu},\text{Dy})$ film after the excitation ceases. The peaks in the curves can be attributed to the ML induced by the impact of the steel ball. It is obvious that the ML intensity exponentially decreases as the decay time increases, which

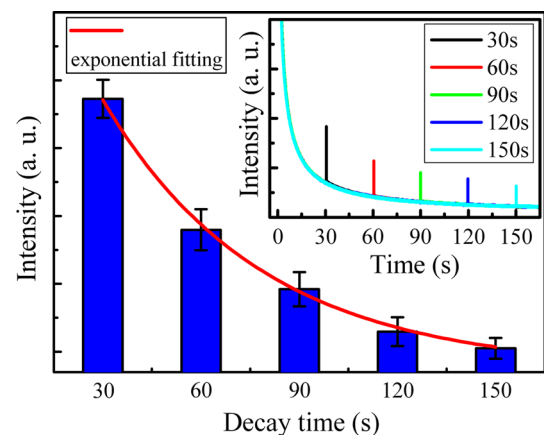


Figure 3 Dependence of impact-induced ML intensity of the $\text{SrAl}_2\text{O}_4:(\text{Eu},\text{Dy})$ film on afterglow decay time. The inset is the typical ML curves of the $\text{SrAl}_2\text{O}_4:(\text{Eu},\text{Dy})$ film after different afterglow decay time.

means that the ML intensity strongly depends on the afterglow decay time of $\text{SrAl}_2\text{O}_4:(\text{Eu},\text{Dy})$ phosphors. So, it is important to consider the decay time as a crucial factor for stress evaluation.

Under controlled conditions, it is feasible to keep the decay time at a certain fixed value to study the relationship between the ML intensity and the impact-induced stress. Figure 4 shows the ML intensity variations with the impact energy, i.e., the steel ball dropped from the different height. In each test, the afterglow decay time before applying the impact on the ML films was fixed at 30 s. At each dropping height, ten tests were carried out to obtain

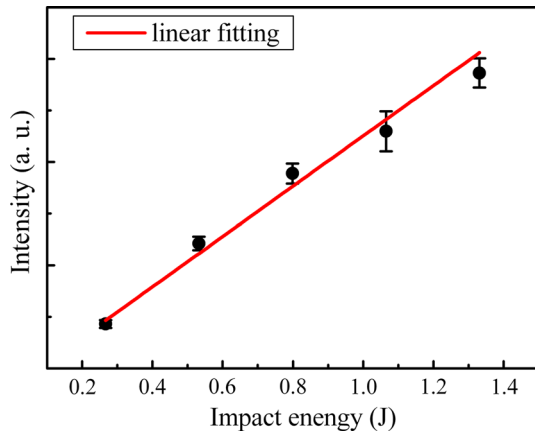


Figure 4 Variations of ML intensity of the $\text{SrAl}_2\text{O}_4:(\text{Eu},\text{Dy})$ film with impact energy. The error is estimated using the standard deviation of the average ML intensity from ten separate drops for each dropping height.

an average ML intensity for the same sample. The ML intensity increases linearly with the impact energy, which is consistent with the results reported in other literatures [26, 27]. This implies that the $\text{SrAl}_2\text{O}_4:(\text{Eu},\text{Dy})$ -based ML films are suitable for sensing the impact stress quantitatively. However, in the real world, the occurrence of an impact is unpredictable. As a result, the decay time of the ML film should be treated as a variant. A much more complicated model should be established to predict the stress from the ML intensity along with the decay time [22].

Here, a practical method is proposed to obtain stable ML irrespective of the decay time. Under continuous UV irradiation, the ML intensity of the $\text{SrAl}_2\text{O}_4:(\text{Eu},\text{Dy})$ film can keep consistent when the film is subject to the same successive impacts. To show the effect of UV irradiation on the impact-induced ML of the $\text{SrAl}_2\text{O}_4:(\text{Eu},\text{Dy})$ film, five stainless steel balls successively dropped from a height of 100 cm onto the $\text{SrAl}_2\text{O}_4:(\text{Eu},\text{Dy})$ film at an interval of 30 s, and the $\text{SrAl}_2\text{O}_4:(\text{Eu},\text{Dy})$ film was irradiated by 365 nm UV LED (voltage = 3.2 V; current = 0.02 A) during the whole process. As shown in Fig. 5, the intensities of the ML induced by five successive impacts are almost at the same level. The baseline of the luminescence curve can be attributed to the photoluminescence of the $\text{SrAl}_2\text{O}_4:(\text{Eu},\text{Dy})$ film excited by 365 nm light source. It is also observed that valleys in the curve appear after the occurrence of ML, due to the $\text{SrAl}_2\text{O}_4:(\text{Eu},\text{Dy})$ film shaded by the steel ball from the UV light during the impacts. For comparison, the impact-induced ML of the

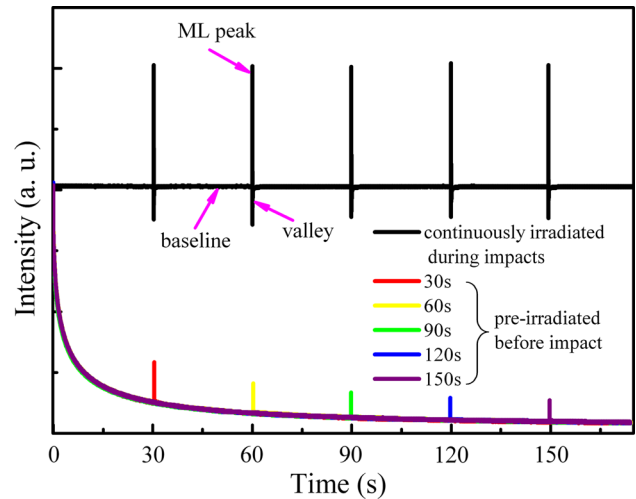
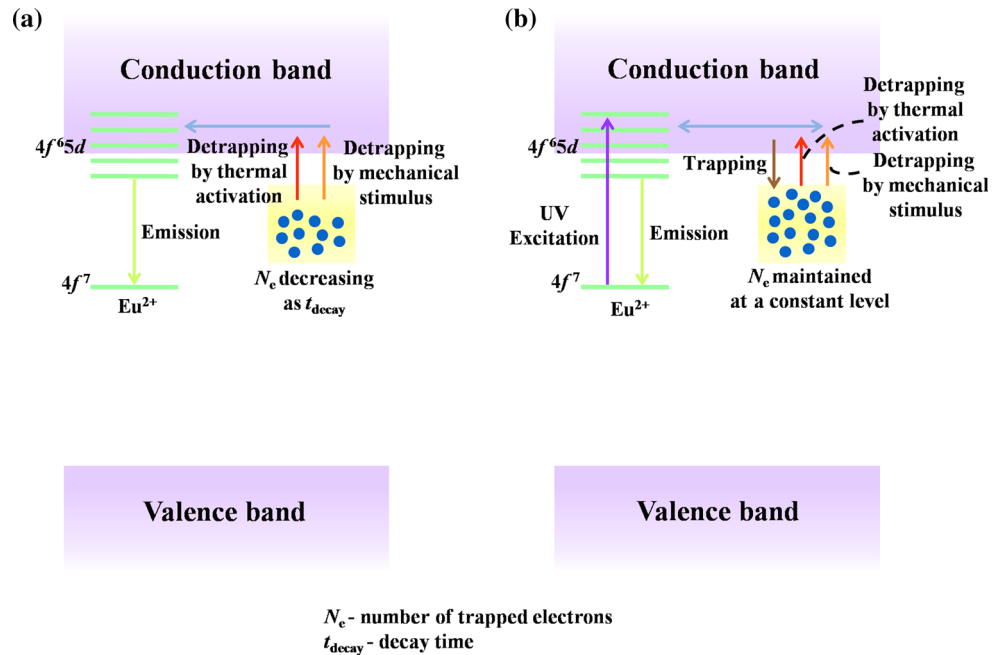


Figure 5 ML curve of the $\text{SrAl}_2\text{O}_4:(\text{Eu},\text{Dy})$ film under continuous UV irradiation and ML curves of the pre-irradiated $\text{SrAl}_2\text{O}_4:(\text{Eu},\text{Dy})$ film after different afterglow decay time.

$\text{SrAl}_2\text{O}_4:(\text{Eu},\text{Dy})$ film after different afterglow decay time is also presented in Fig. 5. In these tests, the $\text{SrAl}_2\text{O}_4:(\text{Eu},\text{Dy})$ films were pre-irradiated for 5 min by 365 nm UV LED (voltage = 3.2 V; current = 0.02 A) and decayed for a certain time before the impact. It is clear that the ML intensity of the $\text{SrAl}_2\text{O}_4:(\text{Eu},\text{Dy})$ film is largely enhanced by the assistance of continuous UV irradiation, compared to the film just with pre-irradiation.

The underlying differences between the ML processes with and without continuous UV irradiation are depicted in Fig. 6. Persistent luminescence and ML of the $\text{SrAl}_2\text{O}_4:(\text{Eu},\text{Dy})$ films are both related to migration of detrapping electrons from traps to Eu^{2+} luminescence center and transition from the 5d level of Eu^{2+} ions to the 4f ground level. However, the way of the electron detrapping in persistent luminescence process is distinct from that in ML process. The release of electrons from the traps in persistent luminescence is assisted by thermal activation or tunneling [28–30] while that in ML involves the piezoelectric field effect induced by the impact [31]. Even though, traps filled with electrons are prerequisite for the occurrence of persistent luminescence or ML. So, the $\text{SrAl}_2\text{O}_4:(\text{Eu},\text{Dy})$ films are needed to be pre-irradiated by UV light to charge the empty traps before measurement of persistent luminescence or ML. After the UV light is off, the $\text{SrAl}_2\text{O}_4:(\text{Eu},\text{Dy})$ films start to exhibit persistent luminescence which consumes the electrons in the traps. As the persistent luminescence decays, the number of electrons in the

Figure 6 Mechanism of ML process **a** without and **b** with UV irradiation.



traps decreases. In the ML theoretical study by Chandra [16], the ML intensity is proportional to the total number of detrappable electrons caught by traps. Therefore, the ML intensity greatly depends on the afterglow decay time. Specifically, the ML intensity decreases as the decay time increases, as shown in the inset of Fig. 3.

Under continuous UV irradiation, four processes, excitation, emission, trapping and detrapping, are involved in the $\text{SrAl}_2\text{O}_4:(\text{Eu},\text{Dy})$ films. At the very beginning of UV irradiation, electrons are excited from the ground state to the excited state of Eu^{2+} ions. A part of them sequentially return back to the ground state, and the other part get trapped. As soon as the electrons get trapped, they can get detrapped and cause afterglow emission. In this period, the trapping of the electrons occurs at a higher rate than the detrapping, so there is a fast buildup of the number of filled traps and an associated increase in the afterglow emission. As a result, the luminescent emission, consisting of photoluminescence emission and afterglow emission, increases as well. After a short period of time (several seconds in our experiment), the intensity of the luminescent emission gets saturated and a steady-state luminescence will be established [32]. Meanwhile, the trapping and detrapping rate of electron will reach equilibrium, which suggests that the number of the trapped

electrons is maintained constant. Thus, the ML intensity can be kept at a stable level.

Figure 7 shows the impact-induced ML variations with the impact energy for the $\text{SrAl}_2\text{O}_4:(\text{Eu},\text{Dy})$ film under continuous 365 nm irradiation. In this experiment, ten tests were carried out to obtain an average ML intensity for the same sample at each dropping height. The ML intensity shows a good linear relationship with the impact energy, which means that

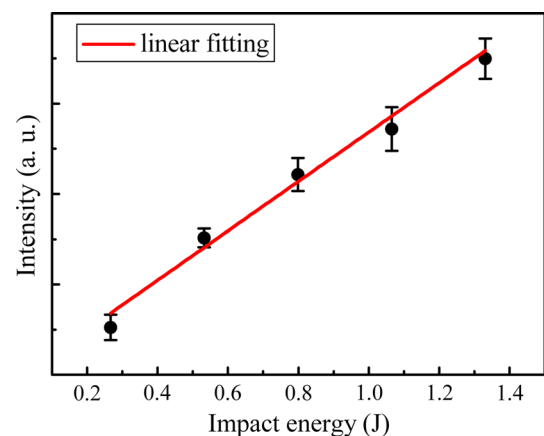


Figure 7 Variations of UV-assisted ML intensity of the $\text{SrAl}_2\text{O}_4:(\text{Eu},\text{Dy})$ film with impact energy. The error is estimated using the standard deviation of the average ML intensity from ten separate drops for each dropping height.

this method has a great potential for quantitative estimation of the impact stress.

Conclusion

The impact-induced ML of $\text{SrAl}_2\text{O}_4:(\text{Eu},\text{Dy})$ has been investigated in this paper. The ML intensity of $\text{SrAl}_2\text{O}_4:(\text{Eu},\text{Dy})$ strongly depends on the afterglow decay time after ceasing the excitation source. Only when the decay time before the occurrence of the impact is kept constant, the ML intensity is proportional to the impact energy. Aiming to achieve a steady-state ML that is not influenced by the decay time, a method is proposed where $\text{SrAl}_2\text{O}_4:(\text{Eu},\text{Dy})$ is continuously irradiated by UV light source during the measurement of ML. Due to the establishment of the equilibrium between trapping and detrapping of electrons in the traps, the number of the trapped electrons is maintained constant. Therefore, stable ML signals can be obtained under continuous UV irradiation. In addition, the ML intensity still linearly correlates with the impact energy, which suggests that this method is beneficial for the application of $\text{SrAl}_2\text{O}_4:(\text{Eu},\text{Dy})$ ML material in impact sensors.

Acknowledgements

This work was supported by the National Natural Science Foundation of China (Grant No. 61372025).

Compliance with ethical standards

Conflict of interest The authors declare that there is no conflict of interest.

References

- [1] Chandra BP (1998) Mechanoluminescence. In: Vij DR (ed) Luminescence of solids. Plenum Press, New York, pp 361–389
- [2] Xu C-N, Zheng X-G, Akiyama M, Nonaka K, Watanabe T (2000) Dynamic visualization of stress distribution by mechanoluminescence image. *Appl Phys Lett* 76:179–181
- [3] Wang XD, Zhang HL, Yu RM et al (2015) Dynamic pressure mapping of personalized handwriting by a flexible sensor matrix based on the mechanoluminescence process. *Adv Mater* 27:2324–2331
- [4] Xu J, Jo H (2016) Development of high-sensitivity and low-cost electroluminescent strain sensor for structural health monitoring. *IEEE Sens J* 16:1962–1968
- [5] Terasaki N, Yamada H, Xu CN (2013) Ultrasonic wave induced mechanoluminescence and its application for photocatalysis as ubiquitous light source. *Catal Today* 201:203–208
- [6] Jeong SM, Song S, Joo KI, Kim J, Hwang SH, Jeong J, Kim H (2014) Bright, wind-driven white mechanoluminescence from zinc sulphide microparticles embedded in a polydimethylsiloxane elastomer. *Energy Environ Sci* 7:3338–3346
- [7] Fang H, Wang X, Li Q, Peng DF, Yan QF, Pan CF (2016) A stretchable nanogenerator with electric/light dual-mode energy conversion. *Adv Energy Mater* 6:1600829
- [8] Sahu IP, Bisen DP, Sharma R (2016) UV excited green luminescence of $\text{SrAl}_2\text{O}_4:\text{Eu}^{2+}$, Dy^{3+} nanophosphor. *Res Chem Intermed* 42:2791–2804
- [9] Chandra VK, Chandra BP (2011) Suitable materials for elastico mechanoluminescence-based stress sensors. *Opt Mater* 34:194–200
- [10] Hollerman WA, Fontenot RS, Bhat KN, Aggarwal MD, Guidry CJ, Nguyen KM (2012) Comparison of triboluminescent emission yields for 27 luminescent materials. *Opt Mater* 34:1517–1521
- [11] Xu CN, Watanabe T, Akiyama M, Zheng XG (1999) Direct view of stress distribution in solid by mechanoluminescence. *Appl Phys Lett* 74:2414–2416
- [12] Yun GJ, Rahimi MR, Gandomi AH, Lim GC, Choi JS (2013) Stress sensing performance using mechanoluminescence of $\text{SrAl}_2\text{O}_4:\text{Eu}$ (SAOE) and $\text{SrAl}_2\text{O}_4:\text{Eu, Dy}$ (SAOED) under mechanical loadings. *Smart Mater Struct* 22:055006
- [13] Someya S, Ishii K, Munakata T, Saeki M (2014) Lifetime-based measurement of stress during cyclic elastic deformation using mechanoluminescence of $\text{SrAl}_2\text{O}_4:\text{Eu}^{2+}$. *Opt Express* 22:21991–21998
- [14] Fu XY, Yamada H, Xu CN (2009) Property of highly oriented $\text{SrAl}_2\text{O}_4:\text{Eu}$ film on quartz glass substrates and its potential application in stress sensor. *J Electrochem Soc* 156:J249–J252
- [15] Kim JS, Kim GW (2014) New non-contacting torque sensor based on the mechanoluminescence of $\text{ZnS}:\text{Cu}$ microparticles. *Sens Actuator A-Phys* 218:125–131
- [16] Chandra BP, Chandra VK, Mahobia SK, Jha P, Tiwari R, Haldar B (2012) Real-time mechanoluminescence sensing of the amplitude and duration of impact stress. *Sens Actuator A-Phys* 173:9–16
- [17] Wang WX, Matsubara T, Takao Y, Imai Y, Xu CN (2009) Visualization of stress distribution using smart mechanoluminescence sensor. *Mater Sci Forum* 614:169–174

- [18] Timilsina S, Lee KH, Kwon YN, Kim JS (2015) Optical evaluation of in situ crack propagation by using mechanoluminescence of $\text{SrAl}_2\text{O}_4:\text{Eu}^{2+}, \text{Dy}^{3+}$. *J Am Ceram Soc* 98:2197–2204
- [19] Azad AI, Rahimi RM, Yun GJ (2016) Quantitative full-field strain measurements by SAOED ($\text{SrAl}_2\text{O}_4:\text{Eu}^{2+}, \text{Dy}^{3+}$) mechanoluminescent materials. *Smart Mater Struct* 25:095032
- [20] Xu C-N (2002) Coatings. In: Schwartz M (ed) *Encyclopedia of smart materials*. Wiley, New York, pp 190–201
- [21] Van den Eeckhout K, Smet PF, Poelman D (2010) Persistent luminescence in Eu^{2+} -doped compounds: a review. *Materials* 3:2536–2566
- [22] Rahimi MR, Yun GJ, Doll GL, Choi JS (2013) Effects of persistent luminescence decay on mechanoluminescence phenomena of $\text{SrAl}_2\text{O}_4:\text{Eu}^{2+}, \text{Dy}^{3+}$ materials. *Opt Lett* 38:4134–4137
- [23] Jha P (2016) Effect of UV irradiation on different types of luminescence of $\text{SrAl}_2\text{O}_4:\text{Eu}, \text{Dy}$ phosphors. *Luminescence* 31:1302–1305
- [24] Altenburg H, Plewa J, Plesch G, Shpotyuk O (2002) Thick films of ceramics, superconducting, and electro-ceramic materials. *Pure Appl Chem* 74:2083–2096
- [25] Haranath D, Sharma P, Chander H (2005) Optimization of boric acid content in developing efficient blue emitting, long persistent phosphor. *J Phys D Appl Phys* 38:371–375
- [26] Jha P, Chandra BP (2013) Impulsive excitation of mechanoluminescence in $\text{SrAl}_2\text{O}_4:\text{Eu}, \text{Dy}$ phosphors prepared by solid state reaction technique in reduction atmosphere. *J Lumin* 143:280–287
- [27] Rahimi MR, Yun GJ, Choi JS (2014) A predictive mechanoluminescence transduction model for thin-film $\text{SrAl}_2\text{O}_4:\text{Eu}^{2+}, \text{Dy}^{3+}$ (SAOED) stress sensor. *Acta Mater* 77:200–211
- [28] Brito HF, Hölsä J, Laamanen T, Lastusaari M, Malkamäki M, Rodrigues LCV (2012) Persistent luminescence mechanisms: human imagination at work. *Opt Mater Express* 2:371–381
- [29] Pan Z, Lu Y-Y, Liu F (2012) Sunlight-activated long-persistent luminescence in the near-infrared from Cr^{3+} -doped zinc gallogermanates. *Nat Mater* 11:58–63
- [30] Han SC, Wang YH, Zeng W, Chen WB (2016) An outlook of rare-earth activated persistent luminescence mechanisms. *J Rare Earth* 34:245–250
- [31] Chandra VK, Chandra BP (2012) Dynamics of the mechanoluminescence induced by elastic deformation of persistent luminescent crystals. *J Lumin* 132:858–869
- [32] Botterman J, Joos JJ, Smet PF (2014) Trapping and detrapping in $\text{SrAl}_2\text{O}_4:\text{Eu}, \text{Dy}$ persistent phosphors: influence of excitation wavelength and temperature. *Phys Rev B* 90:085147